

# Quantitatively identical orientation-dependent ionization energy and electron affinity of diindenoperylene

Cite as: Appl. Phys. Lett. **103**, 253301 (2013); <https://doi.org/10.1063/1.4850531>

Submitted: 15 November 2013 . Accepted: 02 December 2013 . Published Online: 16 December 2013

W. N. Han, K. Yonezawa, R. Makino, K. Kato, A. Hinderhofer, R. Murdey, R. Shiraishi, H. Yoshida, N. Sato, N. Ueno, and S. Kera



View Online



Export Citation



CrossMark

## ARTICLES YOU MAY BE INTERESTED IN

[Electron affinity of pentacene thin film studied by radiation-damage free inverse photoemission spectroscopy](#)

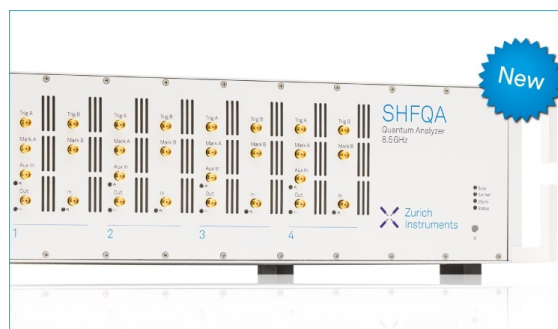
Applied Physics Letters **103**, 123303 (2013); <https://doi.org/10.1063/1.4821445>

[Correlation between interface energetics and open circuit voltage in organic photovoltaic cells](#)

Applied Physics Letters **101**, 233301 (2012); <https://doi.org/10.1063/1.4769360>

[Two-layer organic photovoltaic cell](#)

Applied Physics Letters **48**, 183 (1986); <https://doi.org/10.1063/1.96937>



## Your Qubits. Measured.

Meet the next generation of quantum analyzers

- Readout for up to 64 qubits
- Operation at up to 8.5 GHz, mixer-calibration-free
- Signal optimization with minimal latency

Find out more



# Quantitatively identical orientation-dependent ionization energy and electron affinity of diindenoperylene

W. N. Han,<sup>1</sup> K. Yonezawa,<sup>1</sup> R. Makino,<sup>1</sup> K. Kato,<sup>1</sup> A. Hinderhofer,<sup>1</sup> R. Murdey,<sup>2</sup> R. Shiraishi,<sup>2</sup> H. Yoshida,<sup>2</sup> N. Sato,<sup>2</sup> N. Ueno,<sup>1,a)</sup> and S. Kera<sup>1,b)</sup>

<sup>1</sup>Graduate School of Advanced Integration Science, Chiba University 1-33 Yayoi-cho, Inage-ku, Chiba 263-8522, Japan

<sup>2</sup>Institute for Chemical Research, Kyoto University, Uji, Kyoto 611-0011, Japan

(Received 15 November 2013; accepted 2 December 2013; published online 16 December 2013)

Molecular orientation dependences of the ionization energy (IE) and the electron affinity (EA) of diindenoperylene (DIP) films were studied by using ultraviolet photoemission spectroscopy and inverse photoemission spectroscopy. The molecular orientation was controlled by preparing the DIP films on graphite and SiO<sub>2</sub> substrates. The threshold IE and EA of DIP thin films were determined to be 5.81 and 3.53 eV for the film of flat-lying DIP orientation, respectively, and 5.38 and 3.13 eV for the film of standing DIP orientation, respectively. The result indicates that the IE and EA for the flat-lying film are larger by 0.4 eV and the frontier orbital states shift away from the vacuum level compared to the standing film. This rigid energy shift is ascribed to a surface-electrostatic potential produced by the intramolecular polar bond ( $>\text{C}^--\text{H}^+$ ) for standing orientation and  $\pi$ -electron tailing to vacuum for flat-lying orientation. © 2013 AIP Publishing LLC. [<http://dx.doi.org/10.1063/1.4850531>]

Organic thin films grow different polymorphs at different preparation conditions and on different substrates, which result in variation of their ionization energies (IEs) that impact the energy level alignment at organic interfaces.<sup>1–7</sup> Many studies have shown that such change in IE exists in various organic systems, for instance pentacene,<sup>8–10</sup> diindenoperylene (DIP),<sup>11–13</sup>  $\alpha,\omega$ -dihexyl-sexithiophene (DH6T),<sup>3</sup> and  $\alpha$ -sexithiophene (6T),<sup>3</sup> copper phthalocyanine (CuPc),<sup>6,14</sup> perylene-3,4,9,10-tetracarboxylic dianhydride (PTCDA),<sup>15</sup> etc. There are various origins of the IE variations, e.g., change in intermolecular interaction<sup>5</sup> and polarization effects<sup>16</sup> due to difference of the crystal structure and molecular packing density, and change in the molecular orientation.<sup>2–4,6,10,12,13,15,17,18</sup> These origins are usually related with each other, it is therefore not easy to find the main origin of the IE variation. This problem also produces a difficulty in designing the organic interfaces. Among various origins, a molecular orientation dependence of IE is attributed to the surface-electrostatic potential produced by intramolecular polar bonds at the surface of an oriented molecular layer.<sup>3,4,17,18</sup> In this case, we expect that electron affinity (EA) also show the same shift as IE depending on whether or not the surface is covered by the polar bonds, while other origins, for example changes in intermolecular interaction and polarization effects due to the crystal structure/molecular packing density difference, should result in a significantly different change between IE and EA, since occupied and unoccupied frontier orbitals have different spatial distributions.<sup>5,16</sup>

Accordingly, it is desired to study both of IE and EA of organic films with, for example, different molecular orientations and examine whether these two values change similarly or not, since the values of IE and EA play crucial roles for

the energy level alignment.<sup>19</sup> Unfortunately, however, the direct relationship between the EA and molecular orientation has not yet been studied experimentally.

In this study, we investigated IE and EA of two particular samples of DIP films with flat-lying and standing-up molecular orientation by ultraviolet photoemission spectroscopy (UPS) and inverse photoemission spectroscopy (IPES).<sup>20</sup> DIP films of flat-lying molecular orientation are grown on graphite (highly oriented pyrolytic graphite: HOPG) and films of standing molecular orientation on SiO<sub>2</sub> substrates, which were already reported by electron scattering/diffraction,<sup>12</sup> UPS,<sup>11–13</sup> near-edge X-ray absorption fine structure (NEXAFS),<sup>13</sup> and scanning tunneling microscopy (STM).<sup>13</sup> We found that the IEs and the EAs of these films show a large shift depending on the molecular orientation by keeping the band gap energy unchanged.

For both UPS and IPES, DIP was *in situ* deposited in ultra-high vacuum (UHV) preparation chamber and directly transferred to the measurement chamber without breaking the vacuum. All measurements were carried out at room temperature (RT). For both UPS and IPES, the substrates were prepared as follows: Freshly cleaved HOPG (ZYA grade by SPI Alliance Biosystems) substrate was annealed in UHV before DIP deposition. For SiO<sub>2</sub> substrates, native oxidized Si(111) (p-type) wafer (Waka Tech. Co. Ltd.) was ultrasonically cleaned by acetone and ultra-pure water, and then treated with UV-ozone before loading into the UHV systems.

He I UPS ( $h\nu = 21.22$  eV) experiments were performed with a home-built *in situ* UHV electron spectroscopy system equipped with a PHOIBOS-HSA100 analyzer, with an energy resolution of 60 meV and an acceptance angle of  $\pm 9^\circ$ .<sup>21</sup> UPS spectra were measured at a light incidence angle of  $45^\circ$  and an electron emission angle of  $0^\circ$  (normal emission). The Fermi level ( $E_F$ ) of the sample was determined by measuring the UPS spectrum of a clean gold surface. The

<sup>a)</sup>uenon@faculty.chiba-u.jp

<sup>b)</sup>kera@faculty.chiba-u.jp

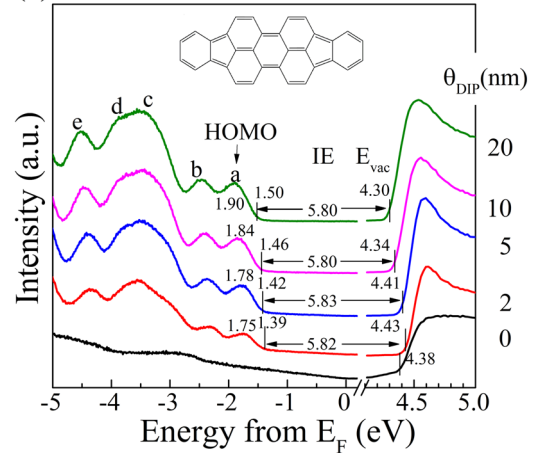
vacuum level ( $E_{vac}$ ) was obtained from the cutoff of secondary electron emission of each UPS spectrum measured by applying a sample bias of  $-5$  V.

IPES was carried out by a home-made *in situ* isochromate spectroscopy mode apparatus<sup>22</sup> with an energy resolution of about  $0.5$  eV, which consists of an e-gun with a BaO coated cathode (PSP Vacuum Technology) and a bandpass detector with the window materials of  $\text{SrF}_2$  and an electron multiplier (Hamamatsu R595) sensitized with KCl layer that can collect the photons in the energy range  $9.4$ – $9.8$  eV. The spectra were acquired by scanning the retarding bias voltage applied to the sample while applying a constant bias of  $-5$  V to the cathode of the electron source. The  $E_F$  was measured from the IPES spectrum of a clean gold surface in order to examine the kinetic energy stability (see below). The  $E_{vac}$  was obtained from the arrest point of second derivative (in this paper the corresponding peak of the first derivative is shown) of the low-energy electron transmission (LEET) spectra by applying  $-5$  V bias to the sample. As kinetic energy of the electron beam (thus work function) depends on condition of the cathode (i.e., the kinetic energy is changed by  $0 \sim 0.2$  eV), it was calibrated by using the work function of each substrate measured by UPS (the  $E_F$  position in the present IPES data).<sup>23</sup>

On the other hand, the work function of  $\text{SiO}_2$  in general shows slightly different values even for similarly treated  $\text{SiO}_2$  substrates and in the present experiments the error in determining the electron energies relative to the  $E_F$  was obtained to  $\pm 0.12$  eV (standard deviation) from UPS measurements of six  $\text{SiO}_2$  substrates. Note that in the present measurements, this error does not exist in EA values but in the  $E_F$  position (origin of the energy scale) of the IPES spectra of DIP/ $\text{SiO}_2$ , since EA is measured from the  $E_{vac}$  at the same cathode condition of the electron gun. Such an error in the  $E_F$  position of energy axis for IPES spectra of DIP/HOPG is  $\pm 0.05$  eV that is much smaller than that for DIP/ $\text{SiO}_2$ .

We first present UPS and IPES spectra of flat-lying DIP deposited on the HOPG in Fig. 1, where Fig. 1(a) shows the thickness ( $\theta_{DIP}$ ) dependence ( $\theta_{DIP} = 2, 5, 10$ , and  $20$  nm) of the UPS spectra of flat-lying DIP thin films for upper valence band and secondary cutoff regions together with the HOPG substrate spectra at the bottom. UPS spectra of the DIP films show five pronounced peaks a, b, c, d, and e for all film thicknesses. The HOMO onset was determined by the method of linear extrapolation of the HOMO slope at low binding energy ( $E_B$ ) side, which is commonly used by many groups, and the peak position was by fitting the HOMO peak with Gaussian functions. The HOMO onset  $E_B$  slightly increases with  $\theta_{DIP}$ . On the other hand, the work function increases from  $4.38$  eV to  $4.43$  eV at  $\theta_{DIP} = 2$  nm, then tends to decrease with further increase in  $\theta_{DIP}$ . We confirmed that at  $\theta_{DIP} = 2$  nm the substrate surface was fully covered by DIP using metastable atom electron spectroscopy (MAES)<sup>24–26</sup> (not shown). For  $\theta_{DIP} \geq 2$  nm, the HOMO onset (also HOMO peak and other peaks) and the  $E_{vac}$  shift in parallel and the HOMO moves away from  $E_F$ . The IE(Th: threshold leading edge) and IE(P: peak), which are defined as the energy difference from HOMO onset and peak to  $E_{vac}$ , respectively, are unchanged at  $5.81 \pm 0.02$  eV and  $6.19 \pm 0.01$  eV in conformity with the reported ones of flat-lying thin film.<sup>12,27,28</sup>

### (a) UPS: DIP/HOPG



### (b) IPES: DIP/HOPG

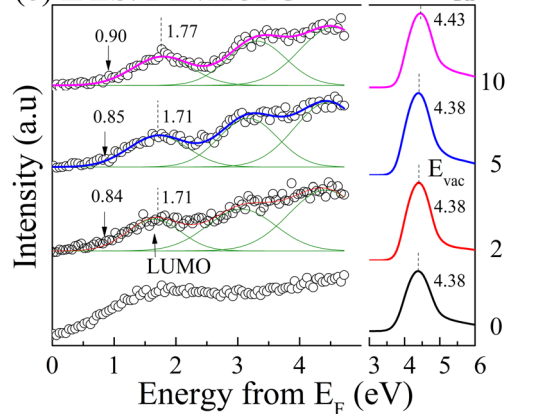


FIG. 1. (a) Thickness ( $\theta_{DIP}$ ) dependence of He I UPS spectra of DIP/HOPG in the HOMO and cutoff regions together with the HOPG substrate spectra at the bottom. The inset shows the molecular structure of DIP. (b) Thickness dependence of IPES spectra of DIP/HOPG. The right part shows the first derivative of the LEET spectra near the vacuum level ( $E_{vac}$ ) (obtained by applying  $-5.0$  V to the sample). All energy values are given in eV.

The thickness dependence ( $2, 5$ , and  $10$  nm) of IPES spectra on DIP/HOPG is shown in Fig. 1(b), where the spectral intensity is normalized by the incidence electron current. The energy positions of spectral features of DIP films are similar independent of the thickness as seen after fitting with Gaussian functions. The LUMO onset (Th: threshold leading edge) was determined by the common method,<sup>10</sup> and the peak position (P: peak) by the fitting curve. The mean value of LUMO onset was obtained to be  $0.86$  eV and that of peak position to be  $1.73$  eV, which gives the EA(Th) and EA(P) that are defined as the energy difference from the LUMO onset and peak to the  $E_{vac}$  are  $3.53 \pm 0.01$  eV and  $2.67 \pm 0.01$  eV, respectively.

The thickness dependences of UPS and IPES spectra for DIP thin films on  $\text{SiO}_2$  are presented in Fig. 2, where the spectrum of the  $\text{SiO}_2$  is also shown at the bottom. As seen in UPS spectra in Fig. 2(a), five pronounced valence band peaks a\*, b\*, c\*, d\*, and e\* are observed for all DIP films, which correspond well with a, b, c, d, and e in Fig. 1(a). The energy positions and relative intensity of the features a\*-e\*, in particular c\* and d\* region, are slightly different from those of the DIP/HOPG, probably due to the different angular distributions of photoelectrons between the films of

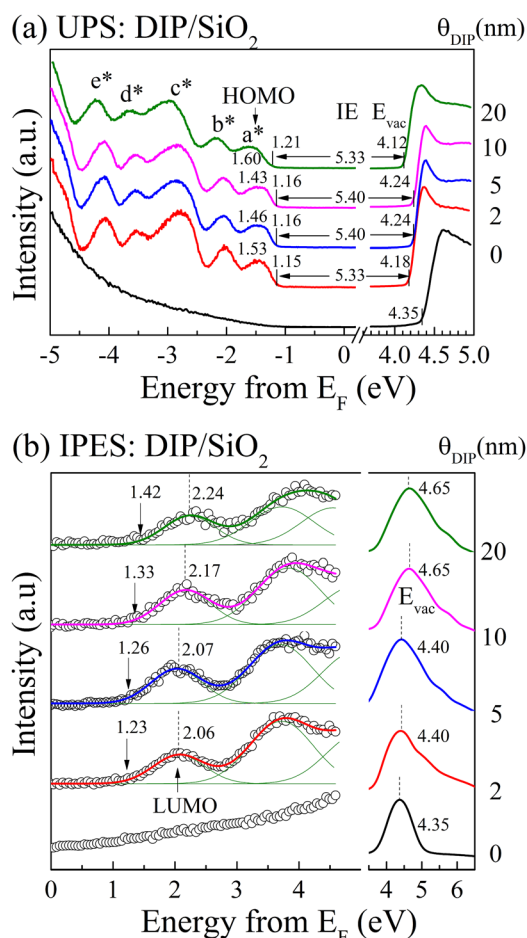


FIG. 2. (a) Thickness ( $\theta_{\text{DIP}}$ ) dependence of He I UPS spectra of DIP/SiO<sub>2</sub> in the HOMO and cutoff regions together with substrate spectra at the bottom. (b) Thickness dependence of IPES spectra of DIP/SiO<sub>2</sub>. The right part shows the first derivative of the LEET spectra near the vacuum level ( $E_{\text{vac}}$ ) (obtained by applying  $-5.0$  V to the sample). All energy values are given in eV.

flat-lying (on HOPG) and standing-up (on SiO<sub>2</sub>) molecules.<sup>28</sup> The HOMO onset  $E_B$  is 1.15–1.16 eV for  $\theta_{\text{DIP}}=2$ –10 nm and becomes 1.21 eV at  $\theta_{\text{DIP}}=20$  nm with clear HOMO tailing into the band gap. The tailing indicates that the 20 nm film involves imperfect molecular packing/crystal structure more than the thinner films. On the other hand, the work function of the bare SiO<sub>2</sub> is 4.35 eV and shifts to 4.18 eV at  $\theta_{\text{DIP}}=2$  nm. For  $\theta_{\text{DIP}}>2$  nm, it first increases slightly to 4.24 eV at  $\theta_{\text{DIP}}=5$  and 10 nm then decreases to reach 4.12 eV at  $\theta_{\text{DIP}}=20$  nm. The trend seems to be resembled to

the HOMO shift. As discussed later, however, the IPES spectrum of the 20 nm film is affected by charging effects, so that we consider that the sudden decrease in the work function (namely  $E_{\text{vac}}$ ) in UPS involves slightly charging effects probably because of increased electron trapping centers due to imperfect molecular packing/crystal structure. Accordingly, we obtain the IE(Th) and IE(P) are  $5.38 \pm 0.04$  eV and  $5.70 \pm 0.01$  eV as the mean values from results for  $\theta_{\text{DIP}}=2$ –10 nm. The thickness dependent shift of the IEs (shown as error) is much smaller than the IE difference between DIP/HOPG and DIP/SiO<sub>2</sub> (see discussion below:  $\Delta\text{IE}(\text{Th})=0.43$  eV,  $\Delta\text{IE}(\text{P})=0.49$  eV). This means that effects of changes in intermolecular interaction and/or polarization effects due to expected tiny changes in molecular packing structure are much smaller than the orientation effects. Both the HOMO onset and the work function slightly shift when the thickness increases as on the HOPG substrate. The IE agrees reasonably with the value of standing DIP thin film.<sup>12,13</sup>

The corresponding IPES spectra are shown in Fig. 2(b) after intensity normalization by the incidence electron current and the energy axis calibration. Two spectral features are clearly seen in each spectrum. The energy positions of LUMO peaks and onsets are the same for 2 and 5 nm DIP films. Note, however, that the LUMO, LUMO+1 peaks and the electron injection peak (of the first derivative curve of LEET) are shifted away from  $E_F$  for the 10 and 20 nm films. This is considered to be caused by the negative charging effect during IPES measurement, since this effect was observed much more after longer data accumulation for thicker films, c.a. 20 nm film. Furthermore, the UPS showed a decrease in the  $E_{\text{vac}}$  [left shift in Fig. 2(a) by positive charging], suggesting that there must be more right-shift in IPES at  $\theta_{\text{DIP}}=20$  nm than that shown in Fig. 2(b). Thus, the charging effect in 20 nm film [Fig. 2(b)] is in part compensated by the decrease in the  $E_{\text{vac}}$  observed by UPS. To be free from influence of the charging effects in determining EA and, in particular, the work function, we use IPES results on 2 and 5 nm films and obtain  $\text{EA}(\text{Th})=3.13 \pm 0.01$  eV and  $\text{EA}(\text{P})=2.31 \pm 0.03$  eV for the DIP film of standing-up molecular orientation.

Accordingly, the molecular orientation-dependent change of IE is obtained as  $\Delta\text{IE}(\text{Th})=0.43 \pm 0.06$  eV and  $\Delta\text{IE}(\text{P})=0.49 \pm 0.02$ , and that of EA as  $\Delta\text{EA}(\text{Th})=0.40 \pm 0.02$  eV and  $\Delta\text{EA}(\text{P})=0.36 \pm 0.03$  eV. These  $\Delta\text{IEs}$

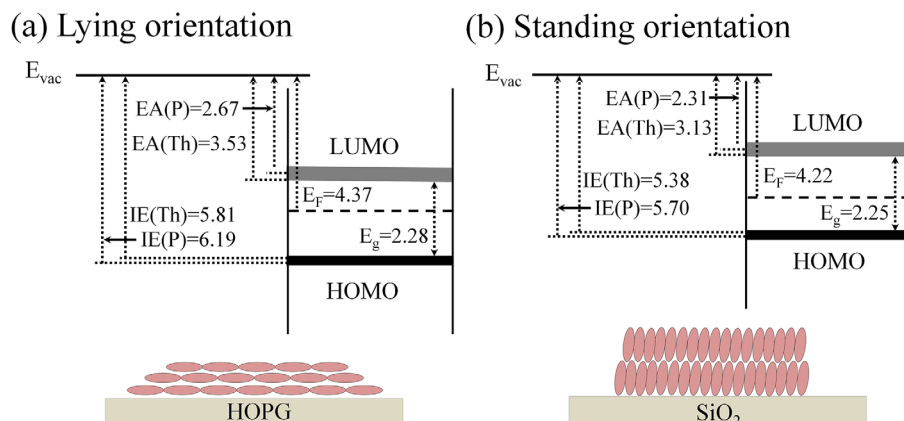


FIG. 3. Schematic molecular-orientation dependence of energy levels of DIP film. (a) Flat lying orientation of DIP on HOPG. (b) Standing up orientation of DIP on SiO<sub>2</sub>. IE(P) and IE(Th) are the ionization energy for HOMO peak and threshold, respectively. EA(P) and EA(Th) are the electron affinity measured with LUMO peak and threshold of LUMO, respectively. The  $E_F$  position (work function) is from the UPS. All energy values are given in eV.



and  $\Delta E_A$ s are much larger than thickness dependent variations of IE and EA. To clearly show the molecular orientation effects, schematics of the energy levels for DIP films of flat-lying and standing-up molecules are shown in Figs. 3(a) and 3(b), respectively, where  $E_F$  is from UPS since the value from IPES has an error of  $\pm 0.12$  eV. In DIP(standing)/SiO<sub>2</sub>, both of HOMO and LUMO thresholds is shifted by  $\sim 0.4$  eV towards  $E_{vac}$ , which makes the IE and the EA smaller than in DIP(flat-lying)/HOPG but the band gap energy is nearly unchanged. The main difference of DIP on HOPG and SiO<sub>2</sub> is that DIP molecular packing orientation is flat-lying and standing-up, respectively. When the surface layer of the films consists of standing-up molecules, the surface electrostatic potential across the  $>C^--H^+$  local-bond layer decreases and thus only the  $E_{vac}$  is decreased,<sup>3,4,17,18</sup> leading to significant lowering ( $\sim 0.4$  eV) of the IE and the EA compared to those of the flat-lying films. An opposite shift of  $E_{vac}$  occurs for the DIP/HOPG system due to  $\pi$ -electron distribution that is spreading outside the surface (molecular plane)<sup>18,26,29</sup> for the flat-lying film, the observed large difference of the IE and EA between DIP/SiO<sub>2</sub> and DIP/HOPG involve both of these contributions, namely,  $>C^--H^+$  local dipole for DIP(standing)/HOPG and opposite-pointing dipole due to  $\pi$ -electron tailing to vacuum for DIP(flat-lying)/HOPG. Thus, values of  $\Delta IE$  and  $\Delta EA$  are changed with the density of the local-bond dipoles at the surface and the size of  $\pi$  conjugation (c.a. number of double bonds in the plane) in the molecule.

In summary, the molecular orientation dependences of ionization energy and electron affinity were studied by UPS and IPES, respectively, for DIP thin films on HOPG and SiO<sub>2</sub> substrates, where the DIP molecular planes are oriented parallel to the surface on HOPG, while molecular long axes are perpendicular to the surface on SiO<sub>2</sub>. For the film of flat-lying DIP, both occupied and unoccupied states shift in parallel away from the vacuum level, which makes IE and EA higher by  $\sim 0.4$  eV comparing to those for the film of standing DIP. The change in these energies, which is dominantly affected by the molecular orientation, is very large and can be reasonably explained by surface local potential produced by the intramolecular polar bond ( $>C^--H^+$ ) and  $\pi$ -electron tailing into vacuum with minor contribution from changes in the molecular packing/crystal structures on graphite and SiO<sub>2</sub> substrates.

This work was financially supported by Global COE program (G-03, MEXT), KAKENHI (Nos. 23360005 and 24245034) and JST PRESTO (Japan Science and Technology Agency, Precursory Research for Embryonic Science and Technology). R.M. and N.S. are grateful for a

partial support by KAKENHI (No. 25410093). A.H. acknowledges support from the JSPS.

- <sup>1</sup>H. Yoshida, K. Inaba, and N. Sato, *Appl. Phys. Lett.* **90**, 181930 (2007).
- <sup>2</sup>W. Chen, H. Huang, S. Chen, Y. L. Huang, X. Y. Gao, and A. T. Wee, *Chem. Mater.* **20**, 7017 (2008).
- <sup>3</sup>S. Duhm, G. Heimel, I. Salzmann, H. Glowatzki, R. L. Johnson, A. J. Vollmer, J. P. Rabe, and N. Koch, *Nature Mater.* **7**, 326 (2008).
- <sup>4</sup>I. Salzmann, S. Duhm, G. Heimel, M. Oehzelt, R. Kniprath, R. L. Johnson, J. P. Rabe, and N. Koch, *J. Am. Chem. Soc.* **130**, 12870 (2008).
- <sup>5</sup>H. Yoshida and N. Sato, *Phys. Rev. B* **77**, 235205 (2008).
- <sup>6</sup>W. Chen, S. Chen, S. Chen, Y. L. Huang, H. Huang, D. C. Qi, X. Y. Gao, J. Ma, and A. T. Wee, *J. Appl. Phys.* **106**, 064910 (2009).
- <sup>7</sup>J. Hwang, A. Wan, and A. Kahn, *Mater. Sci. Eng. R.* **64**, 1 (2009).
- <sup>8</sup>F. Amy, C. Chan, and A. Kahn, *Org. Electron.* **6**, 85 (2005).
- <sup>9</sup>H. Fukagawa, H. Yamane, T. Kataoka, S. Kera, M. Nakamura, K. Kudo, and N. Ueno, *Phys. Rev. B* **73**, 245310 (2006).
- <sup>10</sup>W. N. Han, H. Yoshida, N. Ueno, and S. Kera, *Appl. Phys. Lett.* **103**, 123303 (2013).
- <sup>11</sup>A. Hinderhofer, A. Gerlach, K. Broch, T. Hosokai, K. Yonezawa, K. Kato, S. Kera, N. Ueno, and F. Schreiber, *J. Phys. Chem. C* **117**, 1053 (2013).
- <sup>12</sup>A. Hinderhofer, T. Hosokai, K. Yonezawa, A. Gerlach, K. Kato, K. Broch, C. Frank, J. Novák, S. Kera, N. Ueno, and F. Schreiber, *Appl. Phys. Lett.* **101**, 033307 (2012).
- <sup>13</sup>Y. L. Huang, W. Chen, H. Huang, D. C. Qi, S. Chen, X. Y. Gao, J. Pflaum, and A. T. Wee, *J. Phys. Chem. C* **113**, 9251 (2009).
- <sup>14</sup>H. Yamane, Y. Yabuuchi, H. Fukagawa, S. Kera, K. K. Okudaira, and N. Ueno, *J. Appl. Phys.* **99**, 093705 (2006).
- <sup>15</sup>W. Chen, D. C. Qi, Y. L. Huang, H. Huang, Y. Z. Wang, S. Chen, X. Y. Gao, and A. T. Wee, *J. Phys. Chem. C* **113**, 12832 (2009).
- <sup>16</sup>N. Ueno, S. Kera, and K. Kanai, in *The Molecule-Metal Interface*, edited by N. Koch, N. Ueno, and A. T. S. Wee (Wiley-VCH, Berlin, 2013), p. 176.
- <sup>17</sup>S. Duhm, S. Hosoumi, I. Salzmann, A. Gerlach, M. Oehzelt, B. Wedl, T. L. Lee, F. Schreiber, N. Koch, N. Ueno, and S. Kera, *Phys. Rev. B* **81**, 045418 (2010).
- <sup>18</sup>G. Heimel, I. Salzmann, S. Duhm, and N. Koch, *Chem. Mater.* **23**, 359 (2011).
- <sup>19</sup>H. Fukagawa, S. Kera, T. Kataoka, S. Hosoumi, Y. Watanabe, K. Kudo, and N. Ueno, *Adv. Mater.* **19**, 665 (2007).
- <sup>20</sup>N. V. Smith, *Rep. Prog. Phys.* **51**, 1227 (1988).
- <sup>21</sup>T. Hosokai, M. Horie, T. Aoki, S. Nagamatsu, S. Kera, K. K. Okudaira, and N. Ueno, *J. Phys. Chem. C* **112**, 4643 (2008).
- <sup>22</sup>N. Sato, H. Yoshida, and K. Tsutsumi, *J. Electron Spectrosc. Relat. Phenom.* **88–91**, 861 (1998).
- <sup>23</sup> $E_F$  and thus the work function of a metal vary due to change in the electron kinetic energy. Therefore, we do not use the  $E_F$  position determined for the gold surface for the origin of the energy axis for IPES spectra because we needed to turn off the cathode heater during changing the specimen. In IPES measurements once the cathode (electron emitter) heater is turned off.
- <sup>24</sup>S. Kera, H. Setoyama, M. Onoue, K. K. Okudaira, Y. Harada, and N. Ueno, *Phys. Rev. B* **63**, 115204 (2001).
- <sup>25</sup>S. Kera, A. Abduaini, M. Aoki, K. K. Okudaira, N. Ueno, Y. Harada, Y. Shirota, and T. Tsuzuki, *J. Electron Spectrosc. Relat. Phenom.* **88–91**, 885 (1998).
- <sup>26</sup>Y. Harada, S. Masuda, and H. Ozaki, *Chem. Rev.* **97**, 1897 (1997).
- <sup>27</sup>S. Krause, A. Schöll, and E. Umbach, *Org. Electron.* **14**, 584 (2013).
- <sup>28</sup>N. Ueno, A. Kitamura, K. K. Okudaira, T. Miyamae, Y. Harada, S. Hasegawa, H. Ishii, H. Inokuchi, T. Fujikawa, T. Miyazaki, and K. Seki, *J. Chem. Phys.* **107**, 2079 (1997).
- <sup>29</sup>X. T. Hao, T. Hosokai, N. Mitsuo, S. Kera, K. Mase, K. K. Okudaira, and N. Ueno, *Appl. Phys. Lett.* **89**, 182113 (2006).